Journal of Materials Chemistry

Cite this: *J. Mater. Chem.*, 2012, **22**, 13153

www.rsc.org/materials

PAPER

Synthesis of Ag@AgBr/AgCl heterostructured nanocashews with enhanced photocatalytic performance *via* anion exchange†

Changhua An,*[a] Jizhuang Wang,[a] Chuan Qin,[a] Wen Jiang,[a] Shutao Wang,[a] Yang Li[b] and Qinhui Zhang*[b]

Received 20th March 2012, Accepted 27th April 2012
DOI: 10.1039/c2jm31736b

Heterostructured Ag@AgBr/AgCl nanocashews have been synthesized by an anion-exchange reaction between AgCl nanocubes and Br^- ions followed by photoreduction. Compared to polyhedral Ag@AgBr nanoparticles, the obtained nanostructures exhibit enhanced photocatalytic activity towards decomposition of organic pollutants, *i.e.*, rhodamine-B (RhB). For example, only 2 min is taken to completely decompose RhB molecules with the assistance of these novel heterostructured nanoparticles under visible light irradiation. Furthermore, the as-synthesized nanocatalyst can be reused 20 times without losing activity, showing its high stability. Interestingly, the novel heterostructured Ag@AgBr/AgCl nanophotocatalyst also shows efficient visible light conversion of CO_2 to energetic fuels, *e.g.* methanol/ethanol. Therefore, the present route opens an avenue to achieve highly efficient visible-light-driven nanophotocatalysts for applications in environmental remediation and resourceful use of CO_2.

Introduction

Heterostructured optoelectronic materials (HOM) with electronically coupled components often display interesting and unique optical and electronic properties, *i.e.*, enlarged absorption region of the solar spectrum, facilitated charge transportation without increasing the rate of charge recombination, and enhanced charge collection efficiency.[1,2] These excellent properties make HOM potential candidates in the field of photocatalysis, which is a promising green means to solve issues of environmental degradation and energy deficiency.

The size and morphology of photocatalysts are well known to have great effects on their adsorption and photocatalytic performance.[3–6] Much effort has been devoted to synthesize semiconductor nanoparticles with different morphologies, including nanotubes,[7,8] wires,[9,10] mesoporous structures,[11,12] and many other shapes,[13] for their specific properties and corresponding potential applications. However, the controlled synthesis of silver halide nanostructures, which are a class of highly efficient visible-light-driven photocatalyst, still remains a challenge. AgCl nanoparticles with cubic,[14] spherical,[15,16] and other irregular shapes have been achieved.[17,18] Recently, Ye and co-workers synthesized AgCl (or AgBr) nanowires,[10] through oxidizing commercial Ag foils in aqueous solution of Fe^{3+}, Cl^- (or Br^-) in the presence of polyvinylpyrrolidone (PVP). Compared with nanoparticles, the nanowires exhibit excellent photocatalytic activities for the decomposition of methyl orange (MO) under visible light illumination. However, despite the progress in the synthesis of heterostructured nanoparticles of various types of materials,[19–22] as far as we know, few attempts have been made at the synthesis of heterostructured AgX nanoparticles with well-defined shapes. Although plasmonic Ag@Ag(Br, I), Ag@Ag(Cl, Br), and Ag@AgCl–AgI photocatalysts have been synthesized *via* the reactions of Ag_2MoO_4 with halide ions,[23,24] the microscale and irregular morphology of the obtained products result in uncertainty for boosting photocatalytic efficiency and understanding the reaction pathway. Therefore, methodological exploitation of nanoparticles of novel shapes will be expected to provide an avenue to construct efficient visible-light-driven nanophotocatalysts.

In this paper, we have synthesized heterostructured plasmonic Ag@AgBr/AgCl nanocashews through coupling a simple anion-exchange reaction between AgCl nanocubes and Br^- ions with visible-light reduction. The as-prepared novel nanostructured material shows intrinsic high adsorption for dye molecules, which is crucial for improved photocatalytic performance. The

[a]*State Key Laboratory of Heavy Oil Processing and Department of Materials Physics and Chemistry, Key Laboratory of New Energy Physics & Materials Science in Universities of Shandong, College of Science, China University of Petroleum, Qingdao, Shandong 266580, P. R. China. E-mail: anchh@upc.edu.cn; Fax: +86-532-86981787*

[b]*State Key Laboratory of Heavy Oil, College of Chemical Engineering, China University of Petroleum, Qingdao, 266580, P. R. China. E-mail: qhzhang@upc.edu.cn*

† Electronic supplementary information (ESI) available: Schematic reaction system for photocatalytic reduction of CO_2; SEM image and EDAX mapping of the as-prepared AgBr/AgCl nanoparticles; SEM images of polyhedral Ag@AgBr and the degradation curves of RhB solution with cashew-like Ag@AgBr/AgCl, polyhedral Ag@AgBr, TiO_2 and without any photocatalyst under visible light irradiation; UV–vis spectra of RhB solution before and after adsorption on the as-prepared Ag@AgBr/AgCl nanophotocatalyst; change of RhB solution as the degradation proceeds; and SEM image of Ag@AgBr/AgCl after recycling reactions. See DOI: 10.1039/c2jm31736b

highly efficient visible-light decomposition of organic pollutants and reduction of CO_2 with the assistance of Ag@AgBr/AgCl nanocashews imply the as-prepared heterostructured nanocomposite can be applied in the fields of environmental remediation and resourceful use of CO_2. To the best of our knowledge, this is the first report of the visible-light conversion of CO_2 to methanol with silver halide nanomaterials.

Experimental

Materials

Silver nitrate ($AgNO_3$), sodium chloride (NaCl), sodium bicarbonate ($NaHCO_3$), sodium bromide (NaBr), ethylene glycol (EG), polyvinylpyrrolidone (PVP), and rhodamine-B (RhB) were purchased from Sinopharm Chemical Reagent Co., Ltd (Shanghai, China). All the reagents were used as received without further purification.

The preparation of Ag@AgBr/AgCl nanoparticles

The AgBr/AgCl nanocomposite was synthesized by an anion-exchange reaction of Br^- ions with AgCl nanocubes, which could be easily achieved using our reported method.[14] In a typical procedure, AgCl nanocubes were firstly dispersed in 10 mL of de-ionized water in the presence of PVP (27.1 mg). After an aqueous solution of NaBr (0.61 mM, 10 mL) was rapidly added, the reaction was continued under vigorous magnetic stirring for about 10 h. The obtained product was rinsed with de-ionized water several times and dispersed in 10 mL of de-ionized water. Then the dispersion was irradiated under visible light for 30 min to convert some Ag^+ ions on the surface region of AgBr/AgCl to Ag^0 species. The solution color changed gradually from light yellow to bluish violet, indicating the production and assembly of Ag nanoparticles on the surfaces of AgBr/AgCl. For comparison, polyhedral Ag@AgBr nanoparticles were also prepared by a similar process except without the anion-exchange reaction.

Characterization

The crystal structure of the samples was examined by X-ray powder diffraction (XRD) on a Philips X'Pert diffractometer with Cu Kα radiation ($\lambda = 0.15418$ nm). The morphology was observed with a Hitachi S-4800 field emission scanning electronic microscopy (FESEM) instrument. The absorbance spectra of the catalyst were measured by a UV–vis spectrometer (UV-2550, Shimadzu) in a range of 230 to 1000 nm. The content of Ag species in the Ag@AgBr/AgCl surface was confirmed by X-ray photoelectron spectra (XPS), recorded on a Perkin-Elmer PHI-5300 spectrometer, using non-monochromatized Mg Kα radiation as excitation source in a vacuum of 10^{-7} Pa. The charge shift correction was made and the C 1s electron binding energy of 284.6 eV was used for calibration of the instrument. The XPS spectra were fitted using a combined polynomial and Shirley-type background function.

Evaluation of photocatalytic performance

The photocatalytic performance of Ag@AgBr/AgCl was evaluated through degradation of RhB dye and reduction of CO_2 using a 300 W Xe arc lamp (PLS-SXE300/300UV) equipped with a UV cut-off filter as the source of visible light.

For degradation of RhB, 10 mL of a water dispersion of the as-prepared Ag@AgBr/AgCl nanocashews was transferred to an aqueous solution of RhB (10 mL, 20 mg L^{-1}). The dispersion was kept in the dark for 1 h under magnetic stirring to reach the adsorption–desorption equilibrium. The degradation of RhB was monitored by UV-vis spectra. After the reaction was completed, centrifuging the solution enabled the Ag@AgBr/AgCl nanoparticles to be collected to catalyze subsequent reactions. For comparison, investigations without photocatalyst, and with polyhedral Ag@AgBr and commercial TiO_2 (P25) were also carried out.

The reduction of CO_2 was performed in a self-made photocatalytic reactor as shown in the ESI (Fig. S1†). Two portions of Ag@AgBr/AgCl nanoparticles were dispersed in 50 mL of sodium bicarbonate aqueous solution (0.1 M) with magnetic stirring in the vessel. Prior to irradiation, CO_2 with a purity of 99% was bubbled through the solution with a rate of 0.7 L min^{-1} for 10 min to remove air and saturate the solution. The reaction was then performed under visible light irradiation ($\lambda \geq 400$ nm), and the temperature was kept at 0 °C by an ice-bath so as to increase the solubility of CO_2. Centrifugation (10 000 rpm) of the reaction mixtures enabled the catalyst to be easily separated from the liquid solution of the samples. The catalyst was collected for use in triggering new reactions. The product in the solution was first qualitatively analyzed by an Agilent GC7890A (FID detector, CP-WAX58 FFAP columns) through observing the chromatographic peaks related to the elution of alcohol and then comparing them with those for an authentic ethanol standard. This identification was then confirmed by a GC/MS-5975C (Agilent, DB-1 capillary columns). The content of alcohol in the products was determined by an Agilent GC7890A. Blank tests under visible light irradiation without the photocatalyst and in the dark with the photocatalyst under the same experimental conditions were also conducted.

Results and discussion

Crystalline phase and surface composition were investigated by X-ray powder diffraction (XRD) and X-ray photoelectronic spectra (XPS), respectively. Fig. 1(A) shows that the sample consists of face-centred cubic (fcc) AgBr (JCPDS card no. 79-0149) and a small amount of AgCl (JCPDS card no. 31-1238), which is caused by incomplete replacement of AgCl by Br^-. Fig. 1(B) demonstrates that metallic Ag nanoparticles (JCPDS card no. 87-0717) have been generated on the surfaces of AgBr/AgCl after photoreduction. The elemental composition, chemical status, and silver content of Ag@AgBr/AgCl were further determined by means of XPS (Fig. 2). Before visible light irradiation, XPS analyses indicate that AgBr/AgCl contained the elements Ag, Cl, Br, and C. The carbon peak is due to adventitious hydrocarbon from the XPS instrument. The elements Ag, Cl, and Br come from the AgBr/AgCl sample. In Fig. 2(A), the two peaks at approximately 367 eV and 373 eV can be ascribed to the binding energies of Ag $3d_{5/2}$ and Ag $3d_{3/2}$, respectively.[23,25,26] The $3d_{5/2}$ and Ag $3d_{3/2}$ peaks can be further divided into two different bands, 367.1 eV, 368.2 eV, 373.1 eV, and 374.3 eV, respectively. The bands at 367.1 eV and 373.1 eV are attributed

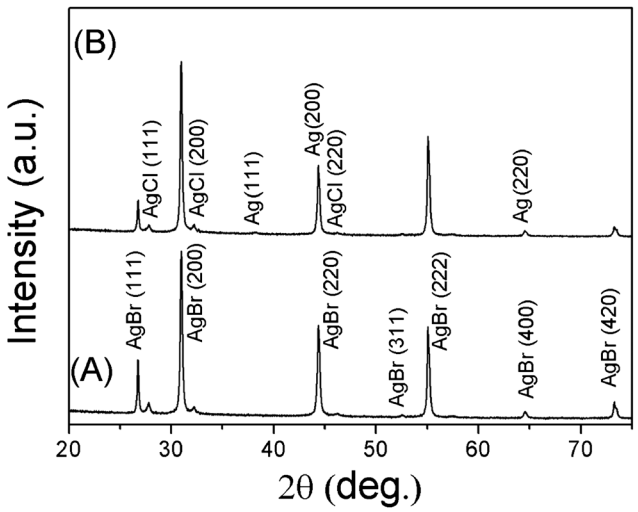

Fig. 1 XRD patterns of (A) AgBr/AgCl and (B) Ag@AgBr/AgCl.

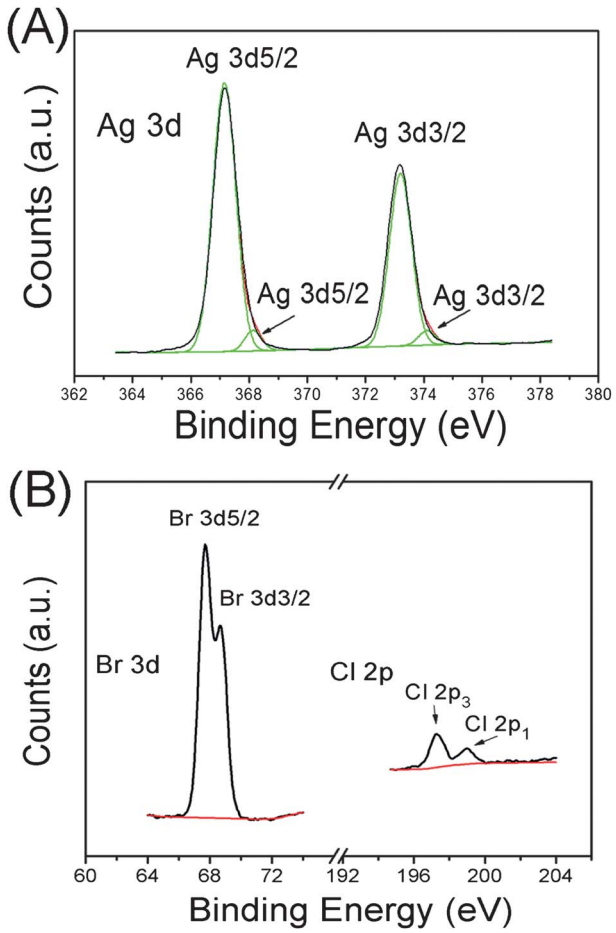

Fig. 2 XPS spectra of the obtained Ag@AgBr/AgCl: (A) Ag 3d; (B) Br 3d and Cl 2p.

to Ag^+, and those at 368.2 eV and 374.3 eV are attributed to metallic Ag^0. The calculated content of surface Ag^0 for the corresponding sample is 7.83 mol%. The spectra of Cl 2p and Br 3d are shown in Fig. 2(B). The binding energies of Cl $2p_{1/2}$ and Cl $2p_{3/2}$ are about 199.0 eV and 197.3 eV, respectively. The spectrum of Br 3d shows that the binding energies of Br $3d_{3/2}$ and Br $3d_{5/2}$ are ~68.7 and ~67.7 eV, in agreement with previous reports.[25] It is noted that the binding energies of both Cl 2p for Cl^- and Ag 3d for Ag^+ shift ~0.6 eV to lower energy, which may be caused by strong interactions between AgCl and AgBr in the as-prepared heterostructures. The calculated surface atomic ratio for Cl, Br, and Ag is 1 : 5.35 : 7.52.

Fig. 3(A) presents typical SEM images of the as-prepared AgCl and Ag@AgBr/AgCl nanoparticles. The AgCl nanoparticles (inset image) display a cubic shape with smooth surfaces. After the ion exchange, highly symmetrical cubic AgCl nanoparticles bound by {100} facets are destroyed. The novel shape of the obtained AgBr/AgCl nanocomposite is that of nanocashews with diameters of 150–300 nm (ESI, Fig. S2†). SEM-EDAX mapping of the sample shown in Fig. 3(A) (ESI, Fig. S3†) confirms the presence of Ag, Br and Cl elements and their distributions in the sample, showing the sample consists of heterostructured nanocashews. Further photoreduction produces plasmonic Ag@AgBr@AgCl nanophotocatalyst, which replicates the same shape as pristine nanoparticles, implying small size and even distribution of the Ag nanoparticles on the surfaces of AgBr/AgCl. Due to the surface plasmonic

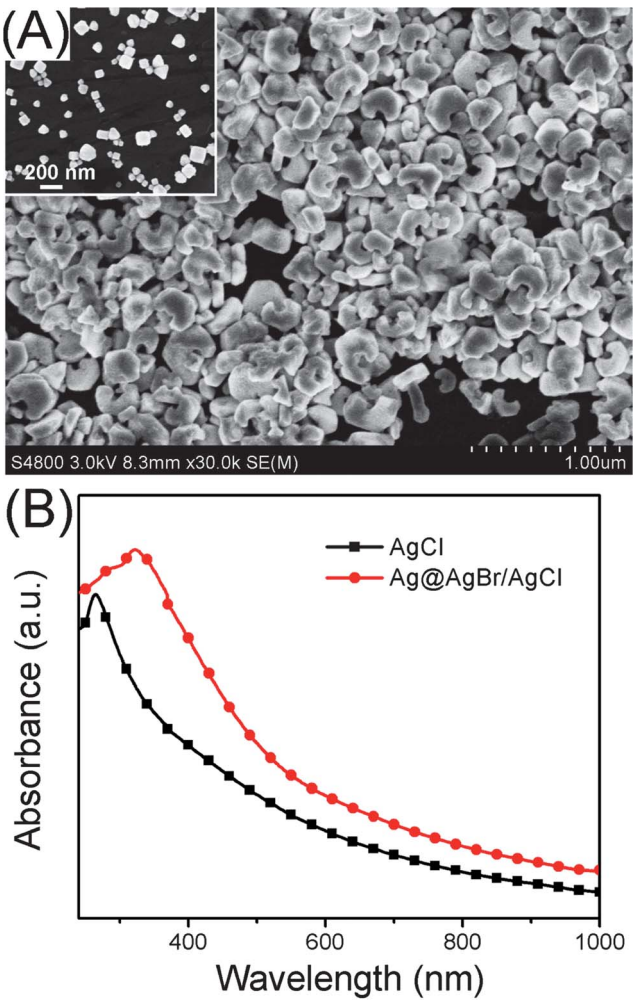

Fig. 3 (A) SEM images of the as-prepared Ag@AgBr/AgCl and (inset) AgCl. (B) UV–vis absorption spectra of AgCl and Ag@AgBr/AgCl.

resonance (SPR) effect of the Ag nanograins, the Ag@AgBr/AgCl nanocashews exhibit a stronger response in the visible region than pristine AgCl nanocubes (Fig. 3(B)).

Based on the SEM investigation of the samples at different stages (Fig. 4), a possible growth mechanism for the conversion of AgCl nanocubes to AgBr/AgCl nanocashews is proposed. At the initial nucleating stage, the anion-exchange reaction was initiated at the corners of the host AgCl nanocubes (Fig. 4b, marked in red circle) due to their high reaction activity. After the AgBr nuclei were produced, they gradually grew up along the near edges of AgCl nanocubes. Then AgBr crystals were slowly wrapped around the host AgCl nanoparticles as the reaction proceeded (Fig. 4c), and the host AgCl nanocubes were transformed into "nanocashews" with the composition of AgBr/AgCl (Fig. 4d). The heterostructured AgBr/AgCl nanostructures with smooth surfaces finally formed through an Ostwald ripening process (Fig. 4e). It can be seen that every nanocashew has a quasi-cubic space surrounded by the backbone structure which should be the trace amount of the host AgCl cubes.

As is known, appropriate adsorption capacity of pollutant molecules on photocatalysts is crucial for the enhancement of catalytic activity.[27–30] Compared to polyhedral Ag@AgBr and commercial TiO_2 (P25), the cashew-like Ag@AgBr/AgCl nanoparticles show a relatively strong adsorption capacity of RhB molecules (ESI, Fig. S4†), which is beneficial for enhancing their photocatalytic activity. Spectral analyses (ESI, Fig. S5†) indicate that 32.9% of RhB molecules are adsorbed on the photocatalyst. Fig. 5(A) shows the evolution of the absorption spectra of RhB with reaction time. The color of RhB solution gradually changes from initially pink to transparent as the reaction proceeds (ESI, Fig. S6†). Therefore, RhB molecules can be decomposed steadily with the assistance of Ag@AgBr/AgCl nanoparticles. However, the degradation of RhB under the same conditions by commercial TiO_2 (P25) and without any photocatalyst was almost nonexistent, confirming the crucial role of Ag@AgBr/AgCl nanoparticles in the bleaching of organic pollutant molecules. Meanwhile, RhB can be completely decomposed within 2 min when catalyzed by Ag@AgBr/AgCl nanocashews, whereas only 94% is decomposed with Ag@AgBr polyhedrons. The relationship between $\ln(C_0/C)$ and irradiation time (t) in Fig. 5(B) is linear, indicating that the reaction follows first-order kinetics with the rate constant determined to be 2.68 min^{-1}.

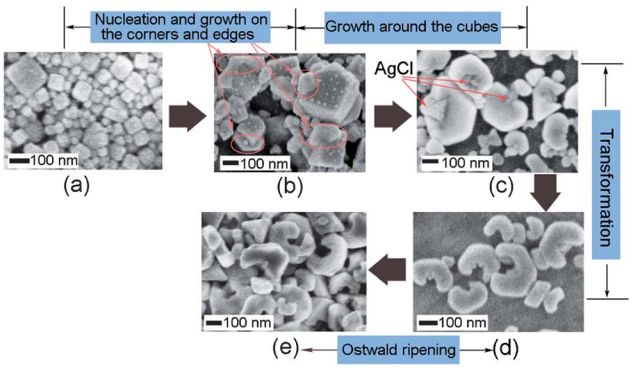

Fig. 4 SEM images for the shape evolution of the samples at different reaction stages: (a) 0 min, (b) 20 min, (c) 60 min, (d) 180 min, and (e) 600 min.

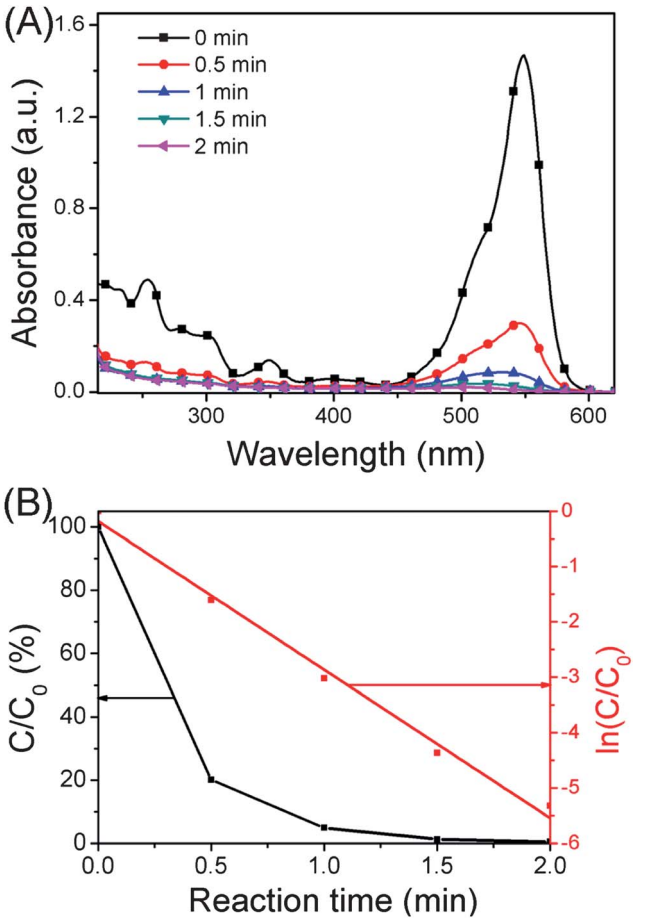

Fig. 5 (A) The change of UV–visible spectra for RhB with the reaction time. (B) The normalized concentration of RhB as a function of reaction time with both linear and logarithmic scales. C_0 is the concentration of RhB before irradiation; C is the concentration of RhB at the reaction time t.

For practical purposes, a photocatalyst should be also stable under repeated use. To evaluate the stability of the present photocatalyst, the Ag@AgBr/AgCl nanoparticles were collected by centrifuging the solution so as to catalyze a new reaction. Fig. 6 shows the degradation kinetics of RhB for 20 reaction runs using the same batch of nanophotocatalyst. The result verifies that the photocatalyst can keep a high efficiency under recycling reactions even though the activity slightly reduces. To a certain extent, the gradual decrease of activity can be attributed to the unavoidable loss of catalyst during the process of sampling and collecting of the photocatalyst. An SEM image of the used photocatalyst (ESI, Fig. S7†) also demonstrates that the microstructure of the nanoparticles is retained well after circulation. Therefore, the as-prepared Ag@AgBr/AgCl nanocashews can be used as a class of highly efficient and stable photocatalyst under visible light irradiation.

Since the amount of carbon dioxide (CO_2) in the global atmosphere has increased as the human race has advanced technologically, there has been growing interest in the development of novel artificial methods that capture and concentrate large quantities of atmospheric CO_2 for subsequent conversion into fuels. Of the many different methods developed so far, the

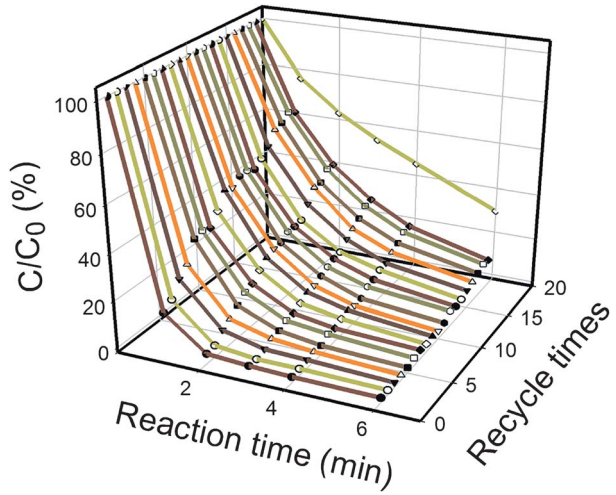

Fig. 6 The degradation curves of RhB solution for 20 successive reactions catalyzed with the same batch of Ag@AgBr/AgCl nanoparticles (as shown in Fig. 1) under visible light irradiation.

reduction of CO_2 with H_2O through irradiation of aqueous suspension systems is regarded as a potential avenue to facilitate CO_2 conversion into useful energy fuels,[31,32] involving a variety of catalytically active semiconductor powders to generate methanol or other organic compounds. However, the pioneering of visible-light-driven photocatalysts for highly efficient CO_2 reduction is still a challenging mission. Herein, we have also evaluated the ability of the present Ag@AgBr/AgCl nanostructure to reduce CO_2 in aqueous solution under visible light irradiation of our self-made system. After reacting for 5 h, GC-MS and GC analyses show that the major products for the reduction of CO_2 are methanol and ethanol. Fig. 7 gives the yield of the photocatalytic products in five reaction runs. The average yields of methanol and ethanol are 226.68 and 329.18 μmol g^{-1}, respectively, which are higher than reported values.[33,34] For each run, the yields of the products do not reduce greatly. Thus the Ag@AgBr/AgCl nanocashews can be applied as a potential candidate for the visible-light reduction of CO_2 with improved efficiency. The high activity of the as-prepared Ag@AgBr/AgCl for CO_2 reduction is attributed to the strong response in the visible region due to the SPR contribution of metallic Ag^0. In addition, the enhanced adsorption capacity may also strengthen the adsorption of CO_2 or CO_3^{2-}, which is helpful for the reduction reaction. Of course, the detailed mechanism is still unclear. A detailed study is needed to give further insight into the conversion pathway.On the basis of the aforementioned results and analyses, a possible mechanism is proposed to explain the high activity and stability of the as-prepared Ag@AgBr/AgCl nanophotocatalyst. The plasmonic absorption of the Ag nanograins (or nanoparticles) in the visible region makes the as-prepared Ag@AgBr/AgCl present an enhanced visible-light response.[17] Under visible light irradiation, the AgBr component with an absorption band at 400–750 nm can be excited by the visible light and produces photogenerated carriers.[35] As a sink for these photoinduced charges, the Ag species on the surfaces of AgBr/AgCl prevents the recombination of photogenerated charges, and thus improves the efficiency of the charge transfer process. Additionally, the well-defined interfaces between Ag and AgBr/AgCl can also improve the rate of interfacial charge transfer. As a result, the photoexcited electrons can be accepted by O_2 adsorbed on the surface of Ag@AgBr/AgCl and form $\dot{O}_2^-$, $\dot{O}H$ and other reactive oxygen species, which would then oxidize RhB molecules.[36,37] The holes will transfer to the surface of AgBr/AgCl to decompose the RhB molecules directly, or oxidize Br^- ions to Br^0 atoms which are also reactive radical species to decompose RhB molecules.[17,38]

In the process for the degradation of RhB, $\dot{O}_2^-$, $\dot{O}H$ and h^+ are supposed to be the main active species. To further elucidate the photocatalytic mechanism and examine the roles of radicals, radical and hole scavengers, including HCO_3^-, *t*-butanol and *p*-benzoquinone, were introduced into the system. As shown in Fig. 8, the degradation of RhB is significantly depressed by the $\dot{O}_2^-$ scavenger *p*-benzoquinone, leading to only 80.7% removal of RhB. However, HCO_3^-, a scavenger of h^+ and the adsorbed $\dot{O}H$, has no obvious influence. Similarly, no significant changes in the degradation are observed with the addition of 0.1 M *t*-butanol

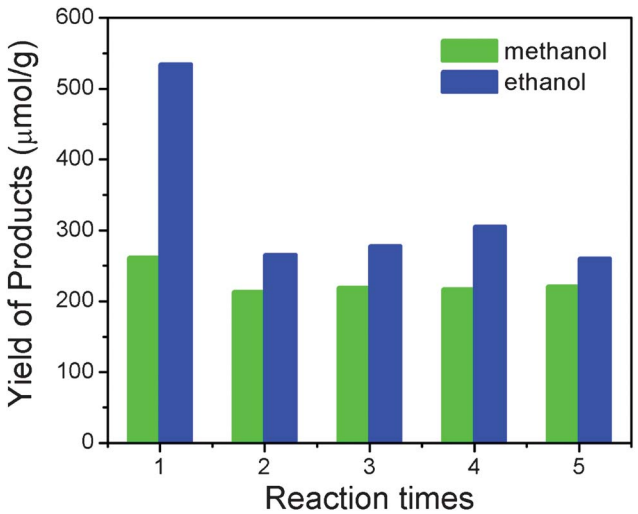

Fig. 7 Yields of photocatalytic products with the number of reaction runs under 5 h visible light irradiation with the same batch of Ag@AgBr/AgCl nanocashews.

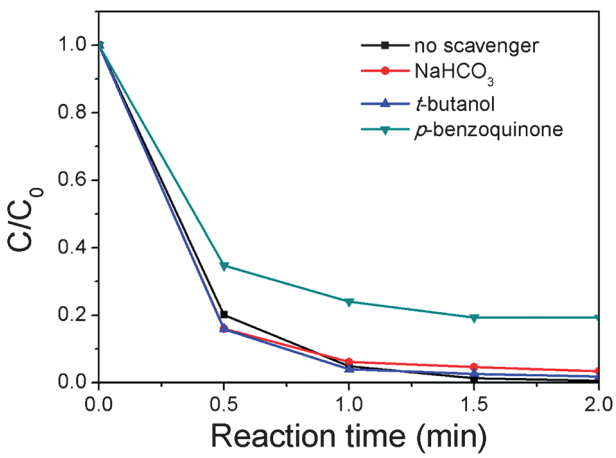

Fig. 8 Photodegradation kinetics of RhB in Ag@AgBr/AgCl water dispersion under visible light irradiation with different scavengers (10 mM $NaHCO_3$, 5 mM *p*-benzoquinone, 0.1 M *t*-butanol).

which predominantly scavenges ·OH in the solution. Hence the $\cdot O_2^-$ radical is the main reactive species in the reaction. The possible process of the degradation of RhB can be proposed as follows. Under visible light irradiation, both the plasmon-induced Ag nanograins and the excited AgBr/AgCl can generate e^-–h^+ pairs. The photoexcited electrons will transfer to the Ag nanograins rather than to the Ag^+ ions of the AgCl lattice, and then the photogenerated electrons will be trapped by O_2 in the solution to form $\cdot O_2^-$ and other oxygen species for the degradation of RhB. Meanwhile, the fast migration of electrons to the surface protects AgBr/AgCl from reduction to Ag, ensuring the high stability of Ag@AgBr/AgCl.

Conclusions

In summary, we have demonstrated a facile anion-exchange process for the synthesis of a cashew-like plasmonic Ag@AgBr/AgCl nanophotocatalyst. The as-prepared photocatalyst exhibits a relatively strong adsorption for dye molecules, which is beneficial for enhancing its photocatalytic activity. RhB molecules can be decomposed completely within 2 min under visible light irradiation. The photocatalyst can be reused 20 times without much decrease of its activity. Furthermore, radical trapping tests confirm that $\cdot O_2^-$ is the main active species in the reaction. In addition, this shaped photocatalyst also displays high activity towards visible-light conversion of CO_2 into fuels, *i.e.* methanol/ethanol. Therefore, the novel cashew-like shape, intrinsic high adsorption, and excellent photocatalytic performance of the heterostructured Ag@AgBr/AgCl photocatalyst make it a promising material in environmental remediation, water disinfection, and resourceful utilization of CO_2.

Acknowledgements

This work is financially supported by the National Natural Science Foundation of China (grant no. 21001116) and the Fundamental Research Funds for the Central Universities (10CX04025A).

Notes and references

1 D. J. Milliron, S. M. Hughes, Y. Cui, L. Manna, J. Li, L. W. Wang and A. Paul Alivisatos, *Nature*, 2004, **430**, 190.
2 C. Mauser, E. Da Como, J. Baldauf, A. L. Rogach, J. Huang, D. V. Talapin and J. Feldmann, *Phys. Rev. B: Condens. Matter Mater. Phys.*, 2010, **82**, 081306.
3 H. Li, Z. Bian, J. Zhu, D. Zhang, G. Li, Y. Huo, H. Li and Y. Lu, *J. Am. Chem. Soc.*, 2007, **129**, 8406.
4 A. Mclaren, T. Valdes-Solis, G. Li and S. C. Tsang, *J. Am. Chem. Soc.*, 2009, **131**, 12540.
5 H. Xu, W. Wang and W. Zhu, *J. Phys. Chem. B*, 2006, **110**, 13829.
6 Y. Bi, S. Ouyang, N. Umezawa, J. Cao and J. Ye, *J. Am. Chem. Soc.*, 2011, **133**, 6490.
7 O. K. Varghses, D. Gong, M. Paulose, K. G. Ong, E. C. Dickey and C. A. Grimes, *Adv. Mater.*, 2003, **15**, 624.
8 T. S. Kang, A. P. Smith, B. E. Taylor and M. F. Durstock, *Nano Lett.*, 2009, **9**, 601.
9 Z. Liu, D. D. Sun, P. Guo and J. O. Leckie, *Nano Lett.*, 2007, **7**, 1081.
10 Y. Bi and J. Ye, *Chem.–Eur. J.*, 2010, **16**, 10327.
11 R. Li, H. Kobayashi, J. Guo and J. Fan, *Chem. Commun.*, 2011, **47**, 8584.
12 F. Zhang, Y. Zheng, Y. Cao, C. Chen, Y. Zhan, X. Lin, Q. Zheng, K. Weia and J. Zhu, *J. Mater. Chem.*, 2009, **19**, 2771.
13 T. D. Nguyen, C. T. Dinh and T. O. Do, *Nanoscale*, 2011, **3**, 1861.
14 C. An, S. Peng and Y. Sun, *Adv. Mater.*, 2010, **22**, 2570.
15 W. Wang, W. Lu and L. Jiang, *J. Colloid Interface Sci.*, 2009, **338**, 270.
16 Z. Lou, B. Huang, P. Wang, Z. Wang, X. Qin, X. Zhang, H. Cheng, Z. Zheng and Y. Dai, *Dalton Trans.*, 2011, **40**, 4104.
17 P. Wang, B. Huang, X. Zhang, X. Qin, H. Jin, Y. Dai, Z. Wang, J. Wei, J. Zhan, S. Wang, J. Wang and M. H. Whangbo, *Chem.–Eur. J.*, 2009, **15**, 1821.
18 H. Xu, H. Li, J. Xia, S. Yin, Z. Luo, L. Liu and L. Xu, *ACS Appl. Mater. Interfaces*, 2011, **3**, 22.
19 C. Wang, C. Xu, H. Zeng and S. Sun, *Adv. Mater.*, 2009, **21**, 3045.
20 Y. W. Jun, J. S. Choi and J. Cheon, *Chem. Commun.*, 2007, 1203.
21 C. Wang, W. Tian, Y. Ding, Y. Q. Ma, Z. L. Wang, N. M. Markovic, V. R. Stamenkovic, H. Daimon and S. Sun, *J. Am. Chem. Soc.*, 2010, **132**, 6524.
22 C. H. Cui, H. H. Li, J. W. Yu, M. R. Gao and S. H. Yu, *Angew. Chem.*, 2010, **122**, 9335.
23 P. Wang, B. Huang, Q. Zhang, X. Zhang, X. Qin, Y. Dai, J. Zhan, J. Yu, H. Liu and Z. Lou, *Chem.–Eur. J.*, 2010, **16**, 10042.
24 P. Wang, B. Huang, X. Zhang, X. Qin, Y. Dai, Z. Wang and Z. Lou, *ChemCatChem*, 2011, **3**, 360.
25 P. Wang, B. Huang, X. Qin, X. Zhang, Y. Dai and M. H. Whangbo, *Inorg. Chem.*, 2009, **48**, 10697.
26 P. Wang, B. Huang, Z. Lou, X. Zhang, X. Qin, Y. Dai, Z. Zheng and X. Wang, *Chem.–Eur. J.*, 2010, **16**, 538.
27 W. Morales, M. Cason, O. Aina, N. R. de Tacconi and K. Rajeshwar, *J. Am. Chem. Soc.*, 2008, **130**, 6318.
28 L. W. Zhang, H. B. Fu and Y. F. Zhu, *Adv. Funct. Mater.*, 2008, **18**, 2180.
29 H. Zhang, X. Lv, Y. Li, Y. Wang and J. Li, *ACS Nano*, 2010, **4**, 380.
30 M. Zhu, P. Chen and M. Liu, *ACS Nano*, 2011, **5**, 4529.
31 T. Inoue, A. Fujishima, S. Konishi and K. Honda, *Nature*, 1979, **277**, 637.
32 S. C. Roy, O. K. Varghese, M. Paulose and C. A. Grimes, *ACS Nano*, 2010, **4**, 1259.
33 K. Kočí, L. Obalová, L. Matějová, D. Plachá, Z. Lacný, J. Jirkovský and O. Šolcová, *Appl. Catal., B*, 2009, **89**, 494.
34 J. Y. Liu, B. Garg and Y. C. Ling, *Green Chem.*, 2011, **13**, 2029.
35 M. Abou Asi, C. He, M. Su, D. Xia, L. Lin, H. Deng, Y. Xiong, R. Qiu and X. Z. Li, *Catal. Today*, 2011, **175**, 256.
36 M. R. Hoffmann, S. T. Martin, W. Choi and D. W. Bahnemann, *Chem. Rev.*, 1995, **95**, 69.
37 A. Houas, H. Lachheb, M. Ksibi, E. Elaloui, C. Guillard and J. M. Herrmann, *Appl. Catal., B*, 2001, **31**, 145.
38 L. Kuai, B. Geng, X. Chen, Y. Zhao and Y. Luo, *Langmuir*, 2010, **26**, 18723.

